FATIGUE CRACK PROPAGATION BEHAVIOR OF THE Al-ALLOY 6013 UNDER VARIABLE AMPLITUDE LOADING IN AN AGGRESSIVE ENVIRONMENT

Hiroyuki SATO*, Gerd LÜTJERING and Albrecht GYSLER

Technical University Hamburg-Harburg, 21071 Hamburg, Germany
*On leave from Tohoku University, Sendai, 980-8579, Japan

ABSTRACT The fatigue crack propagation behavior of the Al-alloy 6013 T6 was studied in 3.5% NaCl solution under variable amplitude loading conditions, including triangular and trapezoidal baseline waveforms (R = 0.1) with superimposed sinusoidal cycles with smaller amplitudes and higher frequencies. Reference constant amplitude curves for different loading frequencies were additionally performed. The results showed that the baseline waveforms and their frequency, as well as the frequency of the superimposed small cycles and their mean stress variations are significantly affecting the crack growth behavior. From an application point of view the most severe variable amplitude loading sequence consisted of a trapezoidal baseline waveform, simulating a ground-air-ground flight cycle, with superimposed small ripples applied during the total baseline cycle period.

Keywords: *Al-alloy 6013, fatigue crack propagation, variable amplitudes, NaCl solution, frequency, hydrogen embrittlement*

1. INTRODUCTION

The Al-alloy 6013 T6 is considered as a prospective candidate to substitute the conventional, damage tolerant alloy 2024 T3 in future aircrafts, for example in skin applications for wings and fuselage [1]. The main advantages of 6013 in comparison to 2024 are a higher resistance against general corrosion and the possibility to reduce production costs by applying welding instead of riveting. For aircraft design purposes as well as for establishing safe inspection intervals, the fatigue crack propagation behavior of the prospective alloy has to be known, preferably under in-service loading conditions [1,2]. The application as skin material for the fuselage, for example, would require a loading sequence consisting of a so-called ground-air-ground cycle (basically a trapezoidal waveform), superimposed by lower amplitude, higher-frequency ripples resulting from vibrations or gust loads.

The purpose of the present study, therefore was to further contribute to the understanding of the fatigue crack propagation behavior under variable amplitude loading, by applying simulated flight loading conditions for one of the proposed applications of the Al-alloy 6013 as skin material for the fuselage of future airplanes.

2. EXPERIMENTAL PROCEDURE

The tests were performed on the commercial Al-alloy 6013 T6 (Al-0.95Mg-0.75Si-0.9Cu-0.35Mn, wt. %), which was supplied as a 1.6 mm thick sheet material. All mechanical tests were carried out at room temperature with the loading axis being parallel to the long transverse direction (T). Tensile properties were determined in air on rectangular test specimens (8 mm width, 40 mm length), using an initial strain rate of $8 \times 10^{-4} s^{-1}$.

Fatigue crack propagation tests were performed on CCT specimens (T-L orientation), with gage dimensions of 30 mm width and 60 mm length. These tests were carried out on a computer controlled servohydraulic testing machine under load control. The aggressive environment consisted of an aqueous 3.5% NaCl solution with an inhibitor of 0.3% Na_2O_7+0.2%Na_2CrO_4 in order to prevent the fracture surfaces from local pitting. All crack growth tests were performed under open circuit conditions at the free corrosion potential. The crack extension was monitored with a travelling light microscope and the average crack length was calculated as a mean value of the two crack length values.

Constant amplitude reference curves were measured at R = 0.1 with a triangular waveform and frequencies of 0.3 and 1 Hz. One type of variable amplitude loading consisted of triangular baseline cycles (R = 0.1, 0.3 Hz) with superimposed sinusoidal ripples of 1.8 Hz or 20 Hz, their ΔK being 22% of the ΔK of the triangular baseline waveform. A second type of variable amplitude loading consisted of a trapezoidal baseline cycle (R = 0.1, 0.15 Hz), having the same ramp slopes as the 0.3 Hz triangular waveform, which resulted in a hold time period of 3.3 sec at maximum load for each baseline cycle. Superimposed on this trapezoidal cycle were sinusoidal ripples with 20 Hz and again a ΔK of 22% of the ΔK of the trapezoidal baseline cycle. These ripples were applied in one case during the hold time period at maximum load only (R = 0.8), and in the other case during the total period of the trapezoidal baseline cycle. The crack propagation rates da/dN for all variable amplitude loading procedures were evaluated on the basis of the baseline cycle counting as one cycle, independently of the number of superimposed ripples, and the concomittant ΔK values were calculated from the maximum and minimum load of the baseline cycle.

Crack closure was monitored by load-displacement curves, obtained by strain gages mounted on both sides of the sheet specimens in front of the propagating fatigue cracks.

3. EXPERIMENTAL RESULTS

The microstructure of the 6013 alloy exhibited a pancake like grain structure with average dimensions along the L-, T- and S-direction of 80 x 60 x 20 μm, respectively. In the peak-aged T6 condition this alloy contains coherent and semi-coherent precipitates. The resulting tensile properties are: $\sigma_{0.2}$ = 345 MPa, UTS = 395 MPa, σ_F = 490 MPa, TE = 14%, RA = 29%.

The fatigue crack propagation curves for the triangular baseline waveforms are summarized in Fig. 1, showing the results for the two constant amplitude tests with 0.3 and 1 Hz, and those for the variable amplitude loading consisting of the 0.3 Hz triangular baseline cycles and superimposed ripples with 1.8 Hz or 20 Hz. The constant amplitude tests exhibited much higher crack growth rates for the 1 Hz as compared to the 0.3 Hz loading frequency. Both of these curves approached each other at high ΔK values of about 20 MPa · $m^{1/2}$ (Fig. 1). The superposition of the 1.8 Hz sinusoidal ripples on the triangular waveform increased the growth rates significantly in comparison to the constant amplitude triangular baseline curve, reaching already at a ΔK of 10 MPa · $m^{1/2}$ the much higher crack growth rates obtained for the 1 Hz triangular waveform. In contrast, the superposition of the 20 Hz ripples resulted at low ΔK in a somewhat lower initial increase in growth rates as compared to that with the 1.8 Hz ripples; however in the higher ΔK regime the growth rates for this variable amplitude sequence was about two times higher in comparison to all three other loading procedures (Fig. 1).

The fatigue crack propagation curves for the two trapezoidal baseline waveforms with superimposed 20 Hz ripples, applied during the hold time at maximum load only as well as during the total period of each baseline cycle, are presented in Fig. 2. Included in Fig. 2 are for comparison reasons the two curves from Fig. 1 for the 0.3 triangular baseline waveforms without and with superimposed 20 Hz ripples. Within the measured ΔK regime the highest crack growth rates of these four loading procedures were obtained for the trapezoidal waveform with the superimposed
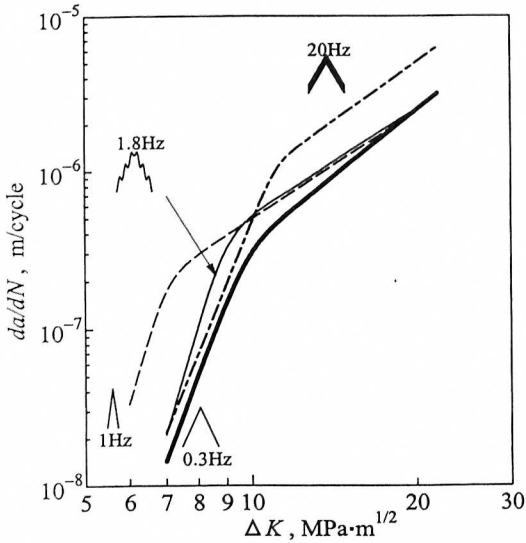
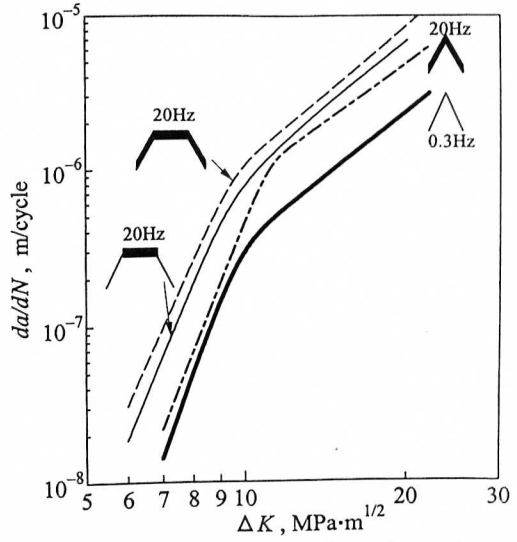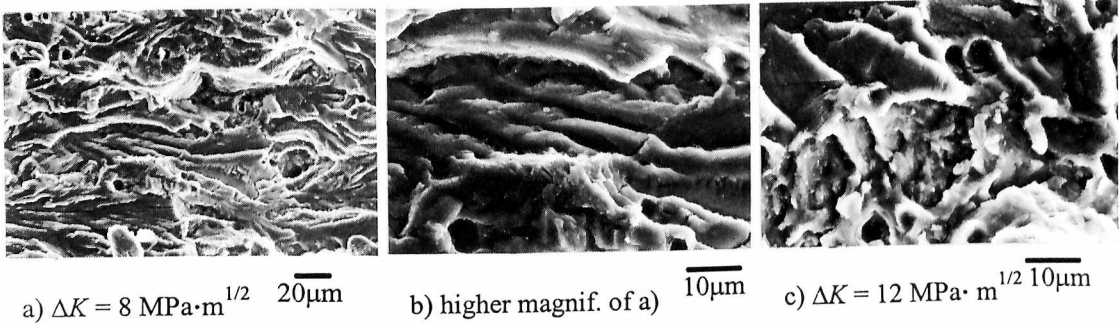Fig. 1: Crack growth rates, triangular baseline waveforms, $R = 0.1$.

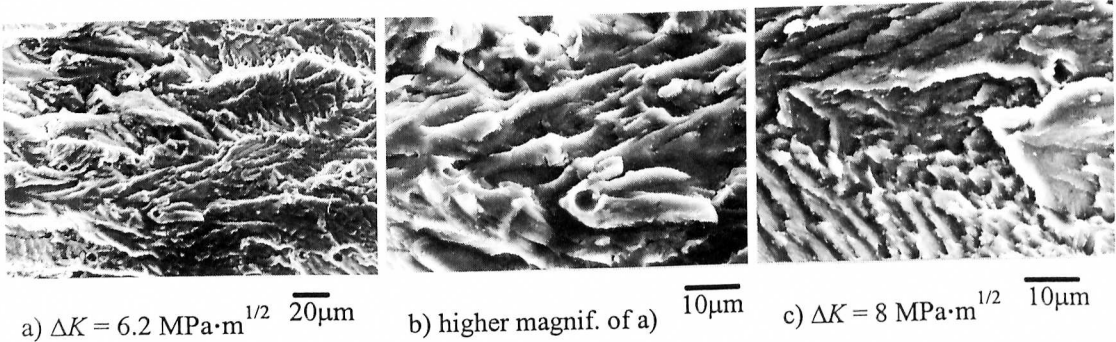Fig. 2: Crack growth rates, triangular and trapezoidal baseline waveforms, $R=0.1$.

⟶ CPD

a) $\Delta K = 8$ MPa·m$^{1/2}$ 20μm   b) higher magnif. of a)   10μm   c) $\Delta K = 12$ MPa· m$^{1/2}$ 10μm

Fig. 3: Fracture surfaces, 0.3 Hz triangular waveform, $R = 0.1$ (SEM).

⟶ CPD

a) $\Delta K = 6.2$ MPa·m$^{1/2}$ 20μm   b) higher magnif. of a)   10μm   c) $\Delta K = 8$ MPa·m$^{1/2}$ 10μm

Fig. 4: Fracture surfaces, 1Hz triangular waveform, $R = 0.1$ (SEM).

a) $\Delta K = 7.5$ MPa·m$^{1/2}$　　10μm

b) $\Delta K = 12$ MPa·m$^{1/2}$　　10μm
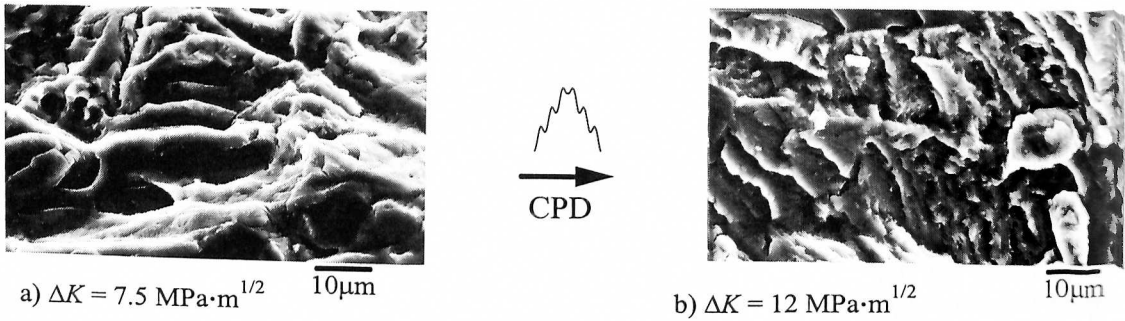
Fig. 5: Fracture surfaces, 0.3 Hz triangular + 1.8 Hz sinusoidal, $R = 0.1$ (SEM).

a) $\Delta K = 7.8$ MPa·m$^{1/2}$　　10μm

b) $\Delta K = 12$ MPa·m$^{1/2}$　　10μm
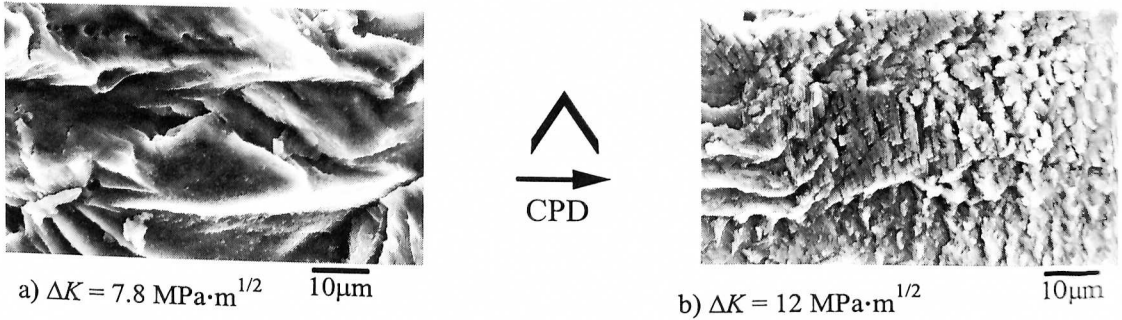
Fig. 6: Fracture surfaces, 0.3 Hz triangular + 20 Hz sinusoidal, $R = 0.1$ (SEM).

a) $\Delta K = 6.6$ MPa·m$^{1/2}$　　20μm

b) higher magnification of a)　　10μm

Fig. 7: Fracture surfaces, 0.15 Hz trapezoidal + 20 Hz sinusoidal, $R = 0.1$ (SEM).

a) $\Delta K = 12$ MPa·m$^{1/2}$　　20μm
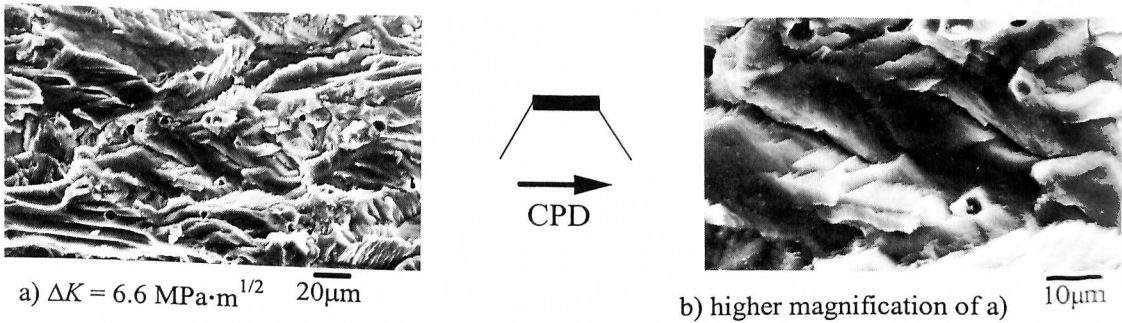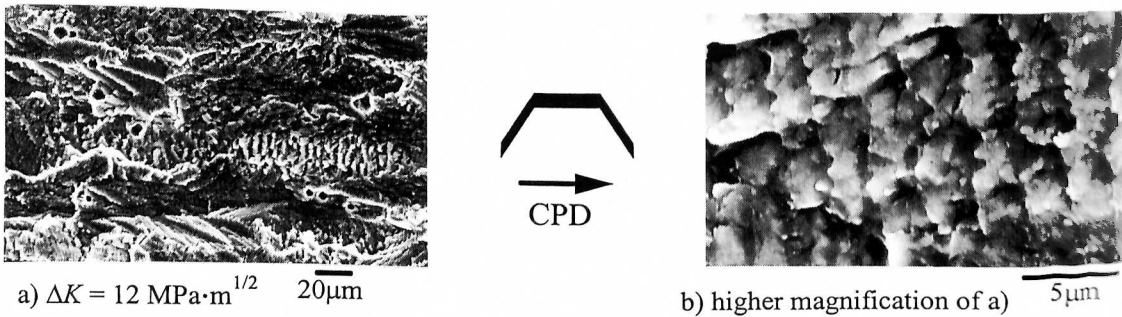
b) higher magnification of a)　　5μm

Fig. 8: Fracture surfaces, 0.15 Hz trapezoidal + 20 Hz sinusoidal, $R = 0.1$ (SEM).

20 Hz ripples applied during the total period of each baseline cycle, followed by the one with the ripples applied during the hold time at maximum load only. The two triangular load sequences (constant and variable amplitudes) showed lower growth rates (Fig. 2).

The measured crack closure levels for all loading procedures applied in the present study were very low, reducing the nominal ΔK values in all cases for less than 10%.

Fracture surface studies revealed exclusively transgranular fracture modes, indepently of loading frequency or waveform. Examples for the constant amplitude triangular loading are shown in Figs. 3 and 4 for applied test frequencies of 0.3 Hz and 1 Hz, respectively. At low ΔK the fracture surface of the 0.3 Hz tested specimen exhibited a ductile appearing fracture mode (Fig. 3a) with microscopically smooth areas elongated in crack propagation direction CPD (Fig. 3b). With increasing ΔK the topography changed gradually to a more brittle appearing mode, showing small facets, while the fraction of smooth areas decreased continuously (Fig. 3c). In contrast, specimens tested with the 1 Hz loading frequency exhibited those smooth and ductile areas only in a very narrow region at the lowest measured ΔK value (Figs. 4a and b). With a slight ΔK increase, coupled with a pronounced increase in growth rate (Fig. 1), the topography changed drastically to a very brittle appearance (Fig. 4c) up to final specimen failure.

The superposition of the 1.8 Hz ripples onto the 0.3 Hz triangular waveform changed the fracture surface from a smooth and ductile appearance at low ΔK (Fig. 5a) by a rather slight increase in ΔK (from 7 to 9.4 MPa $\cdot$ m$^{1/2}$) to a brittle mode (Fig. 5b), similar as observed for the specimen tested with 1 Hz (compare Figs. 4 and 5). Increasing the frequency of the superimposed ripples from 1.8 to 20 Hz, resulted in a somewhat more gradually occurring transition from the observed smooth and ductile appearing topography (Fig. 6a) to a completely brittle fracture mode (Fig. 6b).

Both of the variable amplitude loading procedures based on the trapezoidal waveform showed in prinicipal similar fracture surface variations with increasing baseline ΔK values. A rather ductile fracture mode with microscopically smooth areas was observed for both conditions at low ΔK (Figs. 7a and b), changing for both conditions with increasing ΔK to a very flat and brittle appearing topography (Fig. 8a). The pronounced striations in Fig. 8a, resulting from the trapezoidal baseline cycles, appeared at higher magnification very rugged and brittle (Fig. 8b). This type of striations was found at high ΔK not only for both specimens tested with the trapezoidal waveforms, but also for that with the 20 Hz ripples superimposed onto the triangular waveform (see Fig. 6b) while all three other applied waveforms resulted in very ductile appearing striations at high ΔK values.

4. DISCUSSION

The fatigue crack propagation behavior in aggressive aqueous environments depends on two opposing time dependent environmentally induced processes at the crack tip: hydrogen embrittlement, caused by the formation of hydrogen atoms at bare metal slip steps and their transport into the plastic zone by moving dislocations and by diffusion. These atoms are lowering the local fracture stress, for example in slip planes, which results in higher growth rates. On the other hand, the concurring repassivation of the bare metal slip steps by the formation of a protective oxide layer tends to prevent the hydrogen formation and therefore reduces crack growth rates. The exact time dependence of both processes is unknown so far. Previous results [3, 4] for 6013 have shown, that under constant sinusoidal loading the fatigue crack growth rates exhibited the highest values for a loading frequency of 1 Hz, while for lower (0.1 Hz) and higher frequencies (20 Hz) the propagation rates were lower. The present results for the two constant amplitude tests with 1 Hz and 0.3 Hz triangular waveforms (Fig. 1) are therefore in agreement with those previous results [3]. Comparisons of concomitant fracture surfaces also showed very similar results as those in the previous study. At a constant ΔK, for example at 8 MPa $\cdot$ m$^{1/2}$, the fracture surfaces for tests with

0.3 Hz revealed very smooth and elongated areas (Figs. 3a and b), which are due to crack growth over longer distances along one slip system because repassivation dominates. Contrary, for tests with 1 Hz the fracture appearance was very brittle (Fig. 4c) and crack growth obviously occurred along locally embrittled slip planes, changing frequently from one slip system to the other because of hydrogen embrittlement. It should be noted that in vacuum such a frequency dependent crack growth behavior was not observed [3].

The superposition of the triangular baseline waveform with the 1.8 Hz ripples resulted at low ΔK in a more rapid crack growth increase as compared to that with the 20 Hz ripples (Fig. 1), which can be explained with the frequency dependent crack growth behavior in NaCl solution as described above. The 1.8 Hz ripples are more damaging as compared to the 20 Hz ripples. The significantly higher crack growth rates at high ΔK for the superimposed 20 Hz in comparison to the 1.8 Hz ripples seem to result mainly from the 10 times higher numbers of superimposed 20 Hz ripples per baseline cycle (Fig. 1), which are contributing to mechanical crack growth.

The fatigue crack growth results for the two variable amplitude loading procedures based on the trapezoidal waveform will be discussed in conjunction with the results of the triangular waveform without and with superimposed ripples (Fig. 2). For all four curves the ramp loading rates were constant and in addition the superimposed ripples had the same frequency of 20 Hz. The additional parameter which has to be considered, however is the variation in mean stress for the superimposed ripples. In the low ΔK regime (below 10 MPa $\cdot$ m$^{1/2}$) a pronounced increase in crack growth rates was found between the curves for the triangular waveform with superimposed ripples and the trapezoidal waveform with ripples applied during maximum load. Since the total number of superimposed load cycles per baseline cycle was the same (67 cycles), the higher crack growth rates for the trapezoidal waveform obviously result from the high mean stress of the applied ripples at maximum load with R = 0.8. The application of superimposed ripples during the total period of the trapezoidal baseline waveform showed a further, however much smaller increase in crack growth rates, similar as the increase observed between the two curves for the triangular waveforms without and with superimposed ripples (Fig. 2). The relatively small crack growth increase resulting from the superimposed ripples applied to the ramps of either the triangular or the trapezoidal waveforms can be explained by the low mean stresses which these small ripples experience in the lower parts of each baseline cycle.

Since the fracture surface topographies were very similar for all specimens tested with the 20 Hz ripples superimposed on the triangular as well as on the trapezoidal waveforms (Figs. 6 to 8), it seems reasonable to explain their concomitant crack propagation curves (Fig. 2) mainly on the basis of a mechanical superposition model. However in order to separate the environmental influence from the purely mechanical contribution of baseline and superimposed ripples on crack propagation, the crack growth curves in inert environment would have to be known for these three variable amplitude loading conditions.

ACKNOWLEDGEMENT

REFERENCES

[1]   H.-J. Schmidt and B. Brandecker: in Fatigue '96, Elsevier Science, Oxford, UK (1996), 643.

[2]   R. J. H. Wanhill: Int. J. Fatigue, 16 (1994), 99.

[3]   I. Trockels, A. Gysler and G. Lütjering: in Fatigue '96, Elsevier Science, Oxford, UK (1996), 655.

[4]   I. Trockels, G. Lütjering and A. Gysler: Materials Science Forum, Vols. 217-222 (1996), 1599.